Interrelation between structural ordering and magnetic properties in bcc Fe-Si alloys

N. I. Kulikov
Institute of High Pressure Physics, Troitsk, Moscow region, 142090, Russia

D. Fristot and J. Hugel
Laboratoire de Physique des Liquides et des Interfaces, 1, B[d] Arago, F-57078 Metz Cedex 03, France

A. V. Postnikov
Theoretische Tieftemperaturphysik, Gerhard Mercator Universität – Gesamthochschule Duisburg, D-47048 Duisburg, Germany
(Received 29 March 2001; revised manuscript received 25 October 2001; published 19 July 2002)

We present *ab initio* calculation results of spin-polarized electronic structure in disordered bcc $Fe_{1-x}Si_x$ alloys, starting from dilute solid solutions of Si in iron up to the composition corresponding to the intermetallic compound Fe_3Si ($x=0.01-0.25$). Moreover, the ordered Fe_3Si was simulated in a (fictitious) B2-like ordered structure and in the (stable) $D0_3$ structure. The self-consistent calculations were performed in the coherent potential approximation making use of the Korringa-Kohn-Rostoker method (KKR-CPA) for disordered case and the tight-binding linear muffin-tin orbital (TB-LMTO) method for intermetallic compounds. In the last case the supercell approach has been utilized in order to take into account the structural defects in the B2-type ordered phase. In particular we have calculated the equilibrium structural properties, magnetic moments, and hyperfine fields at iron positions and have explained an instability in the B2-type ordering as compared to the $D0_3$ structure.

DOI: 10.1103/PhysRevB.66.014206 PACS number(s): 71.23.−k, 75.25.+z, 75.50.Bb, 62.20.Dc

I. INTRODUCTION

One of the reasons why the Fe-Si system is traditionally studied over years is the possibility to tune its magnetic properties. Local magnetic moments at Fe sites may become higher than in pure iron, depending on the distribution of Fe and Si neighbors, and finally disappear at Si concentration of nearly 50 at. %.

The phase diagram (see, e.g., Ref. 1) includes in the low-temperature (magnetic) region on the Fe-rich side three ordered structures, which separate different mixed phases, namely pure α-Fe, Fe_3Si of the $D0_3$ type and the cubic (type B20, space group $P2_13$) ϵ-phase FeSi. Since both α-Fe and Fe_3Si have (neglecting the difference in chemical species) the bcc structure, the Fe-Si solid solution up to 25 at. % Si is a bcc substitutional alloy. The difference between the α phase and the α_1 phase (i.e., a solid solution based on the $D0_3$ structure) is merely the degree of ordering. As Si concentration increases, Fe atoms show a certain site preference, preventing the pairs of Si atoms to occupy neighboring positions in the lattice. The α-α_1 boundary is estimated to pass near 10 at. % Si for temperatures below 400°C and is shifted to slightly higher Si concentrations at more elevated temperatures.

The presence of the Si neighbors lowers the average magnetic moment at the Fe site, resulting at the same time in the appearance of high-spin and low-spin Fe species. This has been studied early[2–6] for ordered and disordered $Fe_{1-x}Si_x$ by neutron diffraction, Mössbauer effect measurements, and pulsed NMR studies.

Near the Fe_3Si stoichiometry (i.e., the ordered $D0_3$ phase) one can refer to the fcc lattice with the lattice constant a two times that of underlying α phase and distinguish between the octahedral B $(a/2\ a/2\ a/2)$ and tetrahedral A, $C\pm(a/4\ a/4\ a/4)$ Fe sites, Si being at the D position at (000). The B site has only Fe atoms as all its eight nearest neighbors, whereas A,C sites have four Fe and four Si neighbors. The neutron diffraction finds the magnetic moments of $2.4\mu_B$ and $1.2\mu_B$ at the B and (A,C) sites, respectively.[2–4] In the iron-rich samples (with Fe substituting part of Si positions) Burch *et al.*[5] were able to further distinguish between (A,C) sites with 4:4, 5:3, and 6:2 distribution of Fe:Si neighbors.

A semiqualitative model describing these differences in Fe magnetic moments (also depending on substitutions in the Fe sublattice) was given by Switendick[7] on the basis of non-spin-polarized band-structure calculation and an assumption of a rigid exchange shift of involved local d levels. A quantitative spin-polarized treatment of the ordered Fe_3Si system followed in 1982 due to Williams *et al.*[8] and provided the Fe magnetic moments equal to $1.36\mu_B$ and $2.48\mu_B$ on $[A,C]$ and B sites, correspondingly, in good agreement with above-mentioned experiments. Cohesive, structural, and magnetic properties of all known ordered Fe-Si compounds as obtained on the basis of state-of-the-art calculations have been recently addressed by Moroni *et al.*[9] This publication includes references to many previous studies.

The variation of magnetic properties with concentration was accessed in a phenomenological model by Niculescu *et al.*[10,11] according to which the moment of Fe on $[A,C]$ sites changes linearly with the average number of iron atoms in their nearest-neighbor shell, and the B-site Fe atoms maintain the magnetic moment of $2.2\mu_B$, as in pure α-Fe. (In reality, the magnetic moment at the B site in Fe_3Si is substantially enhanced over the value in the pure Fe.) This model was revised by Elsukov *et al.*[12] for a broader concentration region in disordered Fe-Si alloys; it was proposed that the Fe mag-

netic moment drops linearly by approximately $0.06\mu_B$ as the first and then the second neighbors of Si type appear among the eight nearest neighbors to a Fe site; the further decrease is faster (but also linear) resulting in the disappearance of magnetic moment for seven Si nearest neighbors. A subsequent discussion on the interplay of local order and magnetic properties can be found in Ref. 13.

The first-principles simulation of a disordered system was done by Kudrnovský *et al.*[14] who applied the coherent-potential approximation (CPA) in combination with the tight-binding linear muffin-tin orbitals method (TB-LMTO,[15]) to the Fe-rich $Fe_{(3+y)}Si_{(1-y)}$ system, where chemical disorder (partial substitution of Si with Fe) was allowed at the D sites in the $D0_3$ structure, (A,C) and B sites being occupied by Fe atoms only. It was demonstrated that the above-mentioned phenomenological model (of linear variation of the Fe $[A,C]$ magnetic moments with the number of nearest Fe neighbors) is indeed consistent with a quantitative theory. Recently, the substitution of Fe in both B and $[A,C]$ positions of Fe_3Si with V was addressed in the Korringa-Kohn-Rostoker (KKR)-CPA study by Bansil *et al.*,[16] with the emphasis on magnetic properties and the energetics of substitution. Experimentally, the mean hyperfine field, isomer shift, and saturation magnetization have been studied in Ref. 12 for a broad range of Si concentrations in disordered crystalline and amorphous Fe-Si alloys. The lattice dynamics in the vicinity of the Fe_3Si composition at elevated temperatures has been studied by inelastic neutron scattering by Randl *et al.*,[17] and discussed in relation to high self-diffusivity observed in slightly off-stoichiometric samples.

In view of large general interest for magnetic and elastic properties of Fe-rich Fe-Si systems it remains peculiar that no theoretical study has been undertaken so far, to our best knowledge, with the use of *ab initio* CPA in the assumption of full substitutional disorder on the bcc lattice. For the Si concentration below 10 at. %, when Si atoms are yet far from forming a pronounced sublattice, it would be certainly an adequate model of an alloy. At larger concentrations this still may be an important limiting case, the other one being a substitutional disorder in D sites of the Fe_3Si lattice only, as was assumed in the CPA study of Ref. 14. The real systems, especially at elevated temperatures, tend to allow some Si substitution beyond the D sublattice.

The objective of the present study is to obtain the electronic structure and analyze the elastic and magnetic properties of the Fe-Si system in the range of concentrations 0–25 at. % of Si. This would supplement earlier CPA studies of Kudrnovský *et al.*,[14] the more so that this latter study used fixed lattice constant over the whole concentration region and did not address the changes in equilibrium lattice spacing, nor in elastic properties. For a comparison, the same properties as for disordered alloys are discussed for end members (bcc Fe and Fe_3Si) on the basis of TB-LMTO calculation results, with the technical aspects of calculation possibly close to those in the KKR-CPA study.

II. DETAILS OF CALCULATIONS

The electronic structure of disordered Fe-Si alloys have been calculated using the fast KKR-CPA technique.[18] The zeros of the KKR-CPA determinant are complex since the matrix is not Hermitian. Hence one has to deal with the KKR-CPA determinant itself as a function of **k** and E. For this reason in Ref. 18 an effective tetrahedron method of the Brillouin-zone integration was developed together with the extrapolation approach in the CPA loop, whereby only few iterations are needed in order to solve the CPA equation on the rectangular contour in the complex energy plane. It was moreover shown in Ref. 18 that for a sufficient accuracy in the charge-density self-consistent procedure involving transition-metal alloys, the f-channel scattering must be taken into consideration. Space-filling overlapping atomic spheres were used (as is also typical in TB-LMTO calculations); the core states were recalculated in each iteration. As a rule, 10–20 iterations are required to get the self-consistency of potentials on conditions when the modified Broyden scheme is used in order to accelerate the convergence. Self-consistency (in electronic charge) was reached for, until the electronic density differences were stable to within 10^{-7}. The KKR-CPA calculation setup was the same as described in more detail in Ref. 19 for the calculations of Fe-Cr and Fe-Mn alloys. The **k** mesh with 506 points in the irreducible part of the Brillouin zone, as used in Ref. 19, has now been extended to 1015 and further to 1785 **k** points in order to check the convergency of the **k**-space integration. However, this had no noticeable effect on the total energy nor on magnetic moments.

The TB-LMTO (Ref. 15) calculations also used space-filling atomic spheres and combined corrections. In this sense, the calculation setup was close to that used in the KKR-CPA calculation. The treatment of core states was fully relativistic; for the valence states all relativistic effects, except the spin-orbit coupling, were included as well.

The exchange-correlation in the local-density approximation (LDA) has been treated according to the Hedin-Lundqvist parametrization[20] for nonmagnetic systems and with spin scaling after von Barth and Hedin[21] for magnetic alloys. Along with the LDA, we applied also the generalized gradient approximation (GGA) in the Perdew-Burke-Ernzerhof scheme[22] for the treatment of disordered alloys. Note that we have done that in the atomic sphere approximation, with space-filling (overlapped) atomic spheres and the charge-density spherically symmetrized inside each atomic sphere prior to calculating the exchange-correlation potential. (We emphasize that no feasible way to go beyond muffin-tin, or atomic sphere, approximation is so far available in the CPA algorithm, to our best knowledge.) These shortcomings may become very serious if the gradients of density have to be evaluated, but the introduction of substitutional disorder effectively compensates for the large part of error thus introduced. This empirical observation will be illustrated by results of the following section.

III. RESULTS

We performed a series of calculations on the disordered bcc $Fe_{1-x}Si_x$ alloy with $x=0.01;0.05;0.7;0.1;0.12;0.15;0.25$. In all cases, more then 20 calculations with different lattice constants have been done in order to find the equilib-

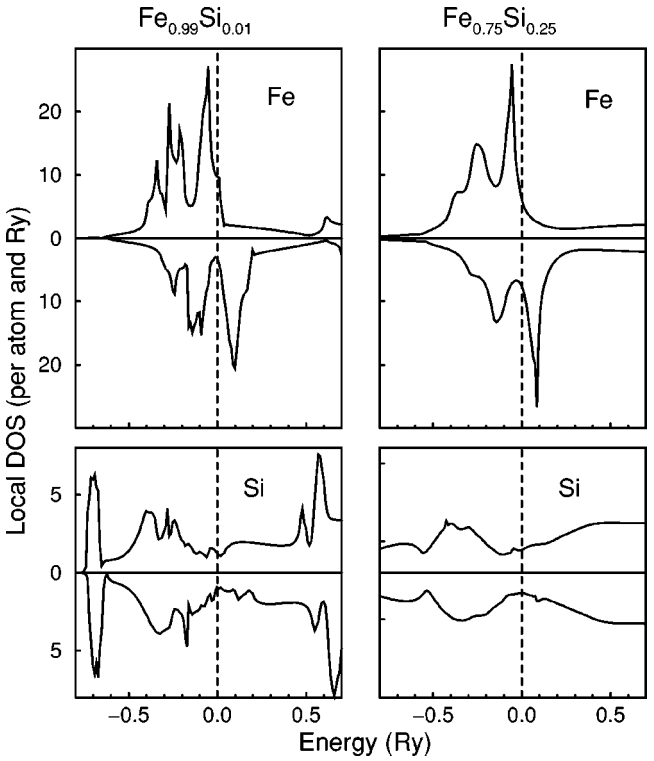

FIG. 1. Spin-resolved local densities of states for two limiting concentrations as calculated by KKR-CPA.

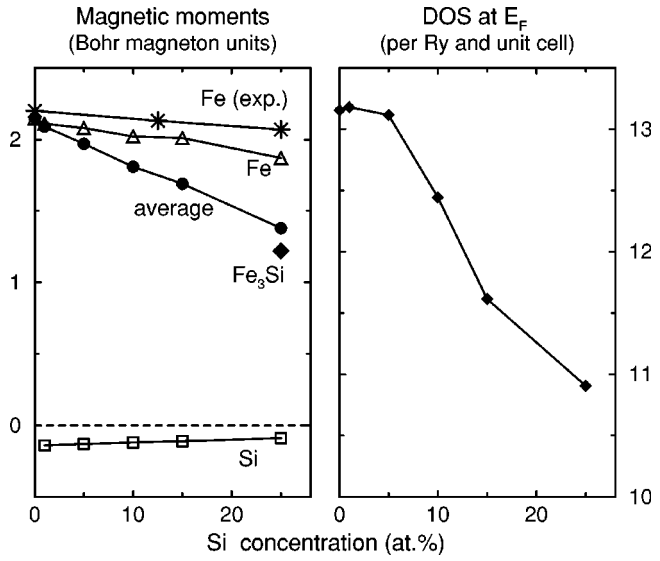

FIG. 2. Calculated electronic properties in dependence on the Si concentration. Left panel: local magnetic moments at Fe and Si sites and mean magnetic moment per atom (the value for ordered Fe_3Si is also shown); right panel: density of states at the Fermi level.

rium atomic space and bulk modulus by the fitting to the Murnaghan equation of state.[23] Moreover, we discuss below the distribution of the density of states (DOS) and magnetic moments at equilibrated lattice constants. For comparison, the same set of results was obtained in TB-LMTO calculations for ordered phases (bcc Fe and Fe_3Si). The electronic structure of these materials is well known and need not to be discussed in detail here. We merely refer to our results for magnetic moments and bulk modulus.

A. Local DOS

The local densities of states (DOS) at Fe and Si sites in two limiting concentrations are shown in Fig. 1. The minimal Si concentration reflects the cases of essentially pure bcc Fe and an isolated Si impurity in Fe, with a typical localized state formed near the bottom of the Fe valence band and the hybridized structure in the energy region of Fe $3d$ bands. Single-impurity calculations with the KKR–Green's-function method give a similar local DOS, e.g., for the Se impurity in Ni.[24] As is generally typical for CPA calculations, the sharp features in the DOS are gradually smeared out at higher concentrations. No other remarkable changes in the DOS could be singled out. One can notice that the position of the Fermi level is near the top of the majority-spin DOS and crossing the minimum between two peaks in the minority-spin DOS remains stable over all concentrations studied, that would imply the stability of a magnetic moment per Fe site. Indeed, the calculated Fe magnetic moment decreases merely from $\sim 2.1\mu_B$ to $\sim 1.9\mu_B$ whereas that at Si sites remains roughly constant at $\sim -0.1\ \mu_B$, resulting in almost linear behavior of the mean magnetic moment per atom with concentration (see Fig. 2, left panel). The slope of the magnetic moment decrease agrees well with the model by Elsukov *et al.*[12] based on experimental data. Again in agreement with the expectations of this model, the calculated average magnetic moment per atom in ordered Fe_3Si falls close to, but lower than, the mean value obtained in the CPA calculation for the $Fe_{0.75}Si_{0.25}$ composition (the corresponding value is shown in the left panel of Fig. 2). Whereas one assumes two Si nearest neighbors to a Fe atom on the average in the disordered case, the mean moment in ordered Fe_3Si combines the contribution from one high-spin (no Si neighbors) Fe(B) atom with twice the contribution of Fe(A, C) atoms, each having four Si neighbors. Note that, as mentioned in the Introduction, the decrease of Fe magnetic moment with the number of Si neighbors is expected to become more rapid for more that two Si neighbors (out of eight in total) appearing to a Fe site.

The value of the mean (per atom) DOS at the Fermi level, $n(E_F)$, decreases with Si concentration as shown in the right panel of Fig. 2, since local $n(E_F)$ at Si sites is lower than that at Fe. The decrease is, however, not linear; it becomes more steep as a narrow plateau in the majority-spin DOS hosting the Fermi level in pure iron gets finally smeared out at ~ 5 at. % Si. From Si concentrations of ~ 15 at. % on, the increase in the minority-spin DOS where the Fermi level rests pinned between two peaks works against the general tendency. In ordered Fe_3Si, $n(E_F)$ is much lower than in the disordered alloy of the same concentration. Qualitatively, this could be seen as an evidence for an ordering tendency in the alloy. The crossover from random distribution of Si atoms over the bcc lattice sites to preferential distribution over D sites of the Fe_3Si structure that happens near 10 at. % Si is not directly addressed in the present study. It could be in-

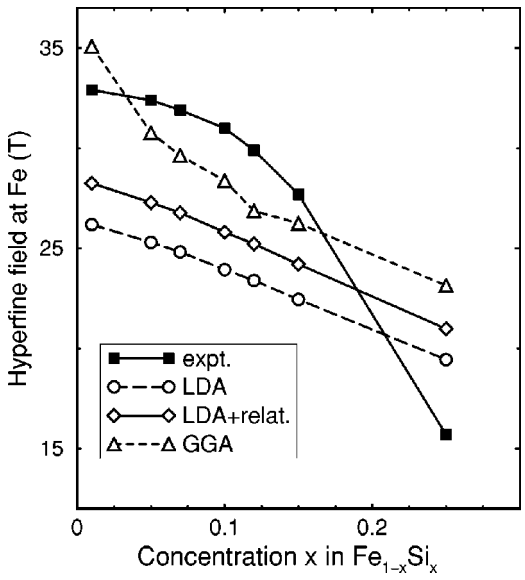

FIG. 3. Measured and calculated in different approximations (see legend and text) hyperfine fields depending on Si concentration.

structive to analyze the total energies in dependence on concentration for both types of disorder in an otherwise similar CPA calculation. Unfortunately, we were not able to treat partial disorder with the computer program presently in use. However we could apply, as an alternative, the supercell approach in the framework of the TB-LMTO method and the results of this simulation will be discussed below.

B. Magnetic properties

Now we present an additional evidence for a significant influence of structural ordering on magnetic properties. In Fig. 3, the calculated values of hyperfine field at iron sites are plotted as function of concentration of Si atoms in disordered alloys. The hyperfine field has as the most important contribution the Fermi contact interaction. In this approximation the hyperfine field is given by the spin density $m(0)$ at nuclear position,

$$m(0)=\int^{E_F} d\epsilon[n_{\uparrow}(0,\epsilon)-n_{\downarrow}(0,\epsilon)].$$

Here $n_{\uparrow,\downarrow}(0,\epsilon)$ are the local DOS for spin-up and spin-down electrons at the nuclear positions. In Fig. 3 we plotted also the results of our nonrelativistic calculations which are far off the experimental values. As was discussed in Ref. 25, in the relativistic case the spin density at the nuclear position has to be replaced by an average of the spin density over the nucleus region with the Thomson radius $r_T=Ze^2/(mc^2)$. It leads to the relativistic enhancement of slightly beyond 7% for Fe, according to Breit and Pyykkö *et al.*[26] (as estimated with hydrogen wave functions).

Let us discuss the experimental and calculated results for hyperfine fields shown in Fig. 3 in some detail. The LDA calculation shows an almost linear (slightly upwards bended) variation of the hyperfine field with concentration. In the experiment, an initial similarly bended almost linear dependency drops down beyond 10 at. % of Si where the effects of ordering on the Fe_3Si lattice start to play a role. Restricting to low Si concentrations, one notices that the absolute values become closer to experiment if relativistic correction is included; even better improvement follows from the use of GGA. Unfortunately, the hyperfine fields calculated with GGA become less regular at exactly these (below 10%) Si concentrations; here an apparent closeness to the experimental values is probably an artifact due to the above-mentioned loss of accuracy in GGA calculations in the low-dilution limit. The dropdown of the measured hyperfine fields from 10 at. % Si on towards 25% can be clearly understood as due to gradually increasing short-range order, that is, an ever growing prominence of the (Fe-enriched) Fe_3Si $D0_3$ lattice, that now competes with the fully disordered bcc alloy. As the $D0_3$ is characterized by the presence of (A, C sites) Fe atoms with enhanced Si coordination and hence lower magnetic moments, the mean hyperfine field decreases faster than linearly with concentration. We argue based on our simulation of a fully disordered alloy that such fast decrease cannot be explained without a partial ordering, that goes along with the phenomenological model used by Elsukov *et al.*[12] to explain their experimental data for hyperfine fields.

C. Lattice parameter and bulk modulus

We turn now to the discussion of elastic properties. The results of the calculations are shown in Fig. 4 in comparison with experimental data (adapted from Ref. 1). The calculated lattice constant changes by less than 0.5% over the whole range of Si concentrations considered. The (half of) lattice constant of the ordered Fe_3Si compound is close to that found for the fully disordered alloy. The experimental measurement over 0–25 at. % Si indicates two linear parts in the concentration dependence of the lattice constant, with a change of slope near 10 at. % Si,[27,28] apparently corresponding to the change from α to α_1 phase. These data are reproduced in Ref. 1 and shown in Fig. 4(a). The alloys prepared by rapid solidification show more smooth change of lattice constant between the two regions.[29] Our calculations also show a smooth change of lattice constant, consistent with the assumption of full substitutional disorder. A systematic underestimation of the lattice parameter a (by $\approx$3%, as compared to experiments) is a typical error in LDA calculations. In order to clarify this point we present in Table I the results for calculations of lattice parameter a and bulk modulus B for pure Fe by different methods within both LDA and generalized gradient approximation (GGA) for the exchange-correlation potential. As one can see, the GGA sets the calculated elastic properties generally closer to experiment, but one should note the loss of precision in the KKR–atomic spheres approximation (-ASA) calculation when using the GGA that was mentioned at the end of Sec. II. Specifically, this gives rise to a certain disagreement between KKR and FP-LAPW results, where the latter do not suffer from this shortcoming.

This observation concerning the comparison of LDA and GGA results to experiment remains valid over a range of

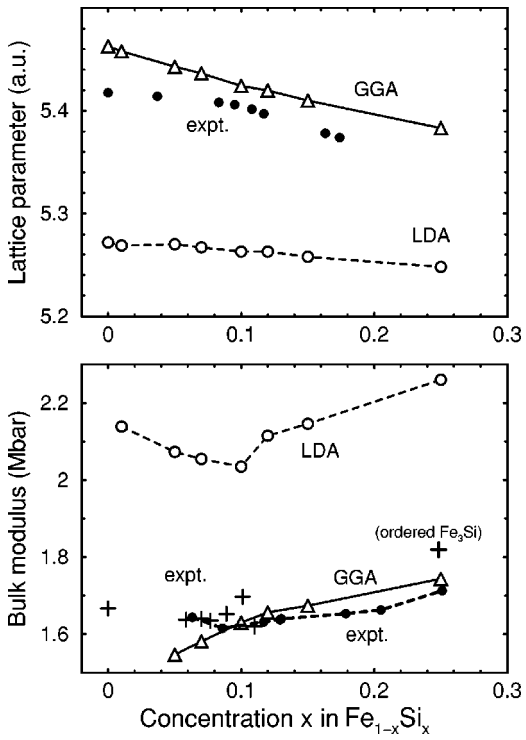

FIG. 4. Calculated (LDA: open circles; GGA: triangles) and measured (black circles, crosses) structure properties depending on Si concentration. Top panel: lattice parameter; bottom panel: bulk modulus. Data are from Ref. 1. Crosses in the bottom panel include data from Refs. 32–34 (also cited in Ref. 1); the connected black circles are recovered from the data of Ref. 31 for the elastic constants. The isolated cross at 24.85% corresponds to the ordered phase.

concentrations as can be seen in Fig. 4, upper panel. Note the augmentation of the GGA error towards low Si concentrations.

The calculated LDA values of the bulk modulus show a dip near 10 at. % Si. Qualitatively, this is consistent with the experimentally observed trend. We failed to find experimental data about the bulk modulus in the sufficiently broad range of Si concentrations; however, room-temperature measurements of elastic constants c_{11} and c_{12} are available in Ref. 31. Along with more limited (in terms of concentration range) data of Refs. 32 and 33 (see also Ref. 1 for a summary) the experimental estimates of bulk modulus as $B=\frac{1}{3}(c_{11}+2c_{12})$ are plotted in Fig. 4. Whereas the strongly nonlinear behavior of c_{11} as function of Si concentration is well documented by the measured data of Ref. 31, the c_{12} values available for several intermediate concentrations seem to be constant. The corresponding values for the bulk modulus recovered from the data of Ref. 31 are shown by connected black circles in the bottom panel of Fig. 4.

TABLE I. Lattice parameter a and bulk modulus B for bcc Fe as calculated by different methods in local-spin density (LDA) and generalized gradient (GGA) approximations.

Method	TB-LMTO	KKR	KKR	FP-LAPW	FP-LAPW	Exp.
Exch. corr.	LDA	LDA	GGA	LDA[a]	GGA[a]	
a, a.u.	5.283	5.272	5.46	5.234	5.401	5.424
B, Mbar	2.10	2.08	1.45	2.44	1.67	1.68

[a]Our benchmark calculations with the Wien97 code (Ref. 30), which agree well with many previous calculations of comparable accuracy.

Thus updated experimental values of the bulk modulus imply a minimum in its concentration dependency at 10 at. %, albeit not so pronounced as in the LDA calculation. What can be the origin of such nonmonotonous change? We know from both experiment and calculation that the lattice constant changes smoothly with concentration; the local magnetic moments, as well as integrated charge density within atomic spheres around both Fe and Si sites, also change unsignificantly between 0 and 25 at. % Si, as is seen from Fig. 2, left panel. On the contrary, the density of states at the Fermi level experiences a drop between 5 and 10 at. % (Fig. 2, right panel), for the reason already explained above. This nonmonotonous change of the density of states apparently has implications on acoustic phonon mode and hence affects the bulk modulus. This effect seems to be of primary electron origin, but the elastic constant c_{11} and consequantly the bulk modulus B are responce functions which normally have the anomaly near phase transition, that would in our case correspond to the inset of partial ordering starting at about the same concentration (10 at. %). It is not possible to obtain a more detailed insight in this interplay of electronic properties and ordering without a straightforward simulation of partially ordered alloys, that seems difficult. One can, however, conclude that the increase in the bulk modulus after 10 at. % of Si is not a simple interpolation toward the ordered Fe_3Si component: the bulk modulus of the latter lays well off (higher than) the smooth concentration-depending trend in disordered alloys, according to both calculations and experiment. Zero-temperature extrapolation of measured bulk modulus is 1860 kbar according to Ref. 34; a slightly lower room-temperature value is indicated by an isolated cross in Fig. 4. Our calculated value of 2600 kbar (in TB-LMTO, using the LDA) or 2483 kbar (with the same method, but including nonlocal correction to exchange-correlation after Langreth and Mehl[36]) remains well above the calculated result for the disordered Fe_3Si alloy, $B=2260$ kbar. (Note that the correction after Langreth and Mehl is not the true GGA, but tends to work in the same direction, usually slightly improving LDA results.) The given ''near-LDA'' numbers are slightly overestimated, but this upward shift is systematic, for both ordered and disordered systems. The full-potential result $B=1990$ kbar reported for Fe_3Si by Moroni *et al.*[9] using the GGA is reasonably close to the experiment.

Unfortunately, applying the GGA for disordered alloys, as was discussed above, faces the problem of accuracy loss at low concentrations (less than 10% of Si, for the system in question). One can see in Fig. 4 how the GGA predictions for the bulk modulus, almost perfect in the range of concentrations 10–25%, start to dramatically deviate from the correct trend (that is set qualitatively correctly by the LDA calculation), ending up with a quite wrong number of B for pure iron (see Table I). Apparently this loss of accuracy

TABLE II. Lattice parameter a, bulk modulus B, magnetic moment M, magnetic energy ΔE_m, and heat of formation H per formula unit of Fe_3Si in $D0_3$ and $B2$-like phases as calculated by the TB-LMTO method.

Structure	a (a.u.)	B (Mbar)	M (μ_B)	ΔE_m (eV/f.u.)	H (eV/at.)
$D0_3$ calc.	10.485	2.60	19.55	−0.54	−0.67
$D0_3$ expt.	10.686[a]	1.86[a]	18.92[b]		−0.21[c]
B2-like	10.461	2.67	16.22	−0.22	−0.55

[a]Reference 34.
[b]Reference 3.
[c]Reference 35.

progresses fast enough to completely absorb the small kink in the concentration dependency of the bulk modulus at 10% Si, that would have been reproduced otherwise in the GGA sequence of data as well.

D. Competing phases for the Fe_3Si composition

The next question to address is the following: Why for the Fe_3Si compound does a more complicated $D0_3$ ordering win over the $B2$? We performed the TB-LMTO calculations for both types of ordering; the results are summarized in Table II. The $B2$ (CsCl)-like ordering was simulated in a supercell approach. If the Si atoms could occupy some B positions (those reserved for Fe atoms in the $D0_3$ structure) and Fe atoms, some D positions, this would result in the $B2$ ordering in the bcc lattice. At the limit of 50% Si we would then obtain the ideal CsCl-type crystal structure. In the case of Fe_3Si we simulated this ordering by interchanging Si(D) and Fe(B) sites.

The calculations show that the magnetic moment at Fe(A, C) dramatically decreases in the presence of an additional (the fifth) Si atom as a nearest neighbor; see Table III. This is in agreement with the phenomenological model of Ref. 12 which predicted exactly the same value of Fe magnetic moments with five Si atoms as nearest neighbors. Iron atoms without nearest Si neighbors maintained their "high-spin" state with magnetic moments equal to, or higher than, that in pure iron and differ only slightly, due to a different number of Fe atoms as second neighbors. (It should be noted that a larger number of Fe atoms in the second shell does not straightforwardly lead to a higher magnetic moment.)

The total magnetic moment per $B2$-like ordered cell is smaller than that in the $D0_3$ structure. This leads to a reduced equilibrium lattice constant as a consequence of smaller negative magnetic pressure. The heat of formation for both lattices is evaluated with respect to the ground state of Fe (ferromagnetic bcc) and Si (diamond structure). As it follows from Table II we obtain the correct stable crystal structure, in agreement with experimental phase diagram. The comparison of magnetic energies (calculated as the energy difference between magnetic and nonmagnetic phases, taken at their respective equilibrium volumes) also shown in Table II indicates that the magnetic component is crucial for establishing the correct energy relation between two phases. The $D0_3$ structure wins because its more sophisticated magnetic structure helps to reduce the total energy more effectively.

We note in passing that the magnetic energy in the $D0_3$ phase has been evaluated by Moroni *et al.*[9] in LDA FP-LAPW calculation, to yield −0.74 eV/cell. The difference from our result can be explained by a different calculation setup. The calculation for the $B2$ structure, however, was not done with the same setup, that would be necessary for an unambiguous comparison of two phases.

The last question we address concerns a possibility for the transition from ferromagnetic (FM) to nonmagnetic (NM) states under pressure in Fe_3Si, that was mentioned in Ref. 37. In Fig. 5 we presented the lattice parameter dependence for total energy of ordered and disordered Fe_3Si as calculated by TB-LMTO and KKR-CPA methods. As the minima for FM and NM phases are shifted apart it seems that the crossover between FM and NM states is at some point possible. However, a closer look at Fig. 5 reveals (see the inset in the left panel) that total-energy curves, instead of crossing, merge together at smaller volumes where the magnetic moment eventually disappears. It is noteworthy that a metamagnetic

TABLE III. Local magnetic moments as calculated by TB-LMTO for $D0_3$ and $B2$-like phases of Fe_3Si (the experimental values, whenever available, are given in parentheses).

Site	1st neighbors	2nd neighbors	M (μ_B)
	$D0_3$		
Fe(A, C)	4Fe(B)+4Si(D)	6Fe(A, C)	1.25 (1.2)
Fe(B)	8Fe(A, C)	6Si(D)	2.47 (2.4)
Si(D)	8Fe(A, C)	6Fe(B)	−0.07 (−0.07)
	B2-type		
Fe(A, C)	2Fe2+Fe1+Si+2Si1+Si2	6Fe(A, C)	0.86
Fe1	8Fe(A, C)	4Fe2+2Si	2.28
Fe2	8Fe(A, C)	2Fe1+2Si1+2Si2	2.56
Fe3	8Fe(A, C)	4Si1+2Si2	2.26
Si	8Fe(A, C)	2Fe1+4Si1	−0.11
Si1	8Fe(A, C)	2Fe2+2Fe3+2Si	−0.05
Si2	8Fe(A, C)	4Fe2+2Fe3	−0.08

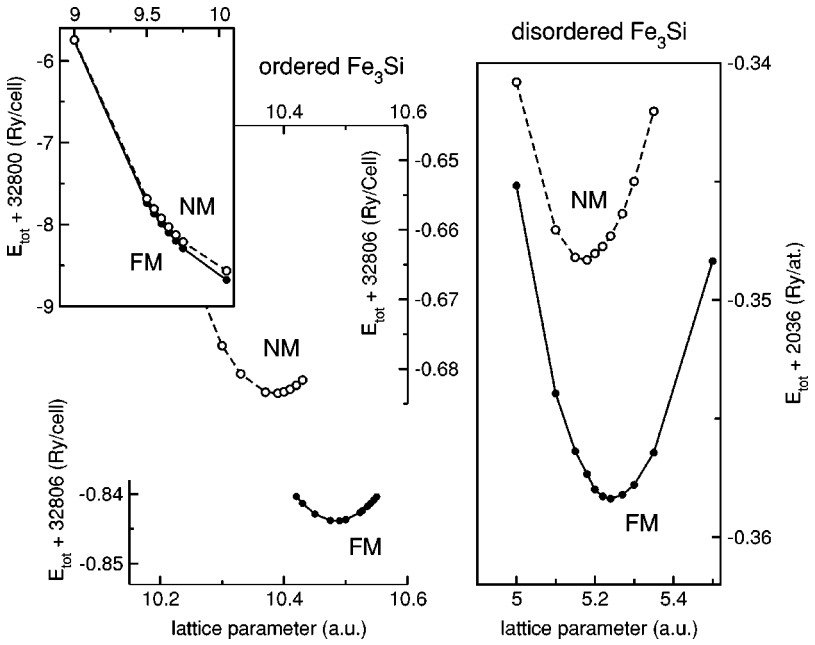

FIG. 5. Total energy as function of volume calculated for ordered $D0_3$ (left panel, TB-LMTO calculation) and fully disordered (right panel, KKR-CPA calculation) cases. The results for ferromagnetic (FM) and nonmagnetic (NM) cases are shown.

behavior with multiple spin solutions for Fe at $A(C)$ sites was found by Christensen *et al.* in the TB-LMTO calculations;[38] moreover, the loss of convergency has been reported for some values of lattice parameter. We performed our TB-LMTO calculations in the lattice parameter range 10.20–10.80 a.u., with a step of 0.05 a.u., and did not find any instability regime. This intriguing behavior demands additional investigations and could have an explanation in the general theory of phase transitions, but the problem is still outside the framework of the present paper.

IV. CONCLUSION

We presented the description of electronic structure and magnetic properties of bcc Fe-Si alloys in the assumption of full substitutional disorder, as treated in the KKR-CPA formalism. Different from earlier CPA studies done in the assumption of partial disorder in the *D* sites of the ordered Fe_3Si compound only, the present study is more adequate in the region of low Si concentrations; moreover, the optimization of lattice spacing and hence the analysis of elastic properties has been done over the range of Si concentrations up to 25 at. %. The changes of bulk modulus with concentration are reported (in agreement with experimental findings) and discussed in terms of evolution of the electronic structure. The calculated results completely confirm the phenomenological model for interrelation between short order and magnetic properties (magnetic moments, hyperfine fields) near Fe_3Si compositions as it follows from disordered alloy KKR-CPA calculations and supercell TB-LMTO calculation for partial ordered compounds.

ACKNOWLEDGMENTS

N.I.K. and A.V.P. are grateful for the hospitality of the University of Metz during their respective stays there, and to N. E. Christensen for useful discussions. A.V.P. acknowledges support from Deutsche Forschungsgemeinschaft (SFB 491).

[1] *Numerical Data and Functional Relationships in Science and Technology*, Landolt-Börnstein, New Series, Group III, Vol. 19, Pt. i1, edited by H. P. J. Wijn (Springer-Verlag, Berlin, 1991).
[2] B. M. Stearns, Phys. Rev. **129**, 1136 (1963).
[3] A. Paoletti and L. Passari, Nuovo Cimento **32**, 25 (1964).
[4] M. B. Stearns, Phys. Rev. B **4**, 4069 (1971).
[5] T. J. Burch, T. Litrenta, and J. I. Budnick, Phys. Rev. Lett. **33**, 421 (1974).
[6] S. Yoon and J. G. Booth, Phys. Lett. **48A**, 381 (1974).
[7] A. C. Swintendick, Solid State Commun. **19**, 511 (1976).
[8] A. R. Williams, V. L. Moruzzi, C. D. Gelatt, Jr., J. Kübler, and K. Schwarz, J. Appl. Phys. **52**, 2019 (1982).
[9] E. G. Moroni, W. Wolf, J. Hafner, and R. Podloucky, Phys. Rev. B **59**, 12 860 (1999).
[10] V. A. Niculescu, T. J. Burch, and J. I. Budnick, J. Magn. Magn. Mater. **39**, 223 (1983).
[11] V. Niculescu *et al.*, J. Phys. Soc. Jpn. **42**, 1538 (1977).
[12] E. P. Elsukov, G. N. Konygin, V. A. Barinov, and E. V. Voronina, J. Phys.: Condens. Matter **4**, 7597 (1992).
[13] A. Arzhnikov, A. Bagrets, and D. Bagrets, J. Magn. Magn. Mater. **153**, 195 (1996).
[14] J. Kudrnovský, N. E. Christensen, and O. K. Andersen, Phys. Rev. B **43**, 5924 (1991).
[15] O. K. Andersen and O. Jepsen, Phys. Rev. Lett. **53**, 2571 (1984); O. K. Andersen, O. Jepsen, and M. Sob, in *Electronic Band Structure and Its Applications: Proceedings, Kanpur, India 1986*, Vol. 283 of Lecture Notes in Physics, edited by M. Yussouff (Springer-Verlag, Berlin, 1987), pp. 1–57.

[16] A. Bansil, S. Kaprzyk, P. E. Mijnarends, and J. Tobol*a*, Phys. Rev. B **60**, 13 396 (1999).
[17] O. G. Randl, G. Vogl, W. Petry, B. Hennion, B. Sepiol, and K. Nembach, J. Phys.: Condens. Matter **7**, 5893 (1992).
[18] A. F. Tatarchenko and N. I. Kulikov, Phys. Rev. B **50**, 8266 (1994).
[19] N. I. Kulikov and C. Demangeat, Phys. Rev. B **55**, 3533 (1997).
[20] L. Hedin and B. L. Lundqvist, J. Phys. C **4**, 2064 (1971).
[21] U. von Barth and L. Hedin, J. Phys. C **5**, 1629 (1972).
[22] J. P. Perdew, K. Burke, and M. Ernzerhof, Phys. Rev. Lett. **77**, 3865 (1996).
[23] F. D. Murnaghan, Proc. Natl. Acad. Sci. U.S.A. **30**, 5390 (1944).
[24] N. Stefanou, A. Oswald, R. Zeller, and P. H. Dederichs, Phys. Rev. B **35**, 6911 (1987).
[25] S. Blügel, H. Akai, R. Zeller, and P. H. Dederichs, Phys. Rev. B **35**, 3271 (1987).
[26] G. Breit, Phys. Rev. **35**, 1447 (1930); P. Pyykkö, E. Pajanne, and M. Inokuti, Int. J. Quantum Chem. **7**, 785 (1973).
[27] M. C. M. Farquhar, H. Lipson, and A. R. Weill, J. Iron Steel Inst., London **152**, 457 (1945).
[28] F. Lihl and H. Ebel, Eisenhüttenw. **32**, 489 (1961).
[29] M. J. Tenwick and H. A. Davies, Int. J. Rapid Solidif. **1**, 143 (1985).
[30] P. Blaha, K. Schwarz, and J. Luitz, Wien97, Vienna University of Technology, 1997, improved and updated Unix version of the original copyrighted WIEN code, which was published by P. Blaha, K. Schwarz, P. Sorantin, and S. B. Trickey, Comput. Phys. Commun. **59**, 339 (1990).
[31] A. Machová and A. Kadečková, Czech. J. Phys., Sect. B **27**, 555 (1977).
[32] H. L. Alberts and P. T. Wedepohl, Physica (Amsterdam) **53**, 571 (1971).
[33] J. L. Routbort, C. N. Reid, E. S. Fisher, and D. J. Dever, Acta Metall. **19**, 1307 (1971).
[34] J. B. Rausch and F. X. Kayser, J. Appl. Phys. **48**, 487 (1977).
[35] F. R. de Boyer, R. Boom, W. C. M. Mattens, A. R. Miedema, and A. K. Niessen, in *Cohesion in Metals: Transition Metal Allloys*, edited by F. R. de Boyer and D. G. Pettifor (North-Holland, Amsterdam, 1988), Vol. 1.
[36] D. C. Langreth and M. J. Mehl, Phys. Rev. Lett. **47**, 446 (1981); Phys. Rev. B **28**, 1809 (1983).
[37] N. E. Christensen, I. Wenneker, A. Svane, and M. Faciulli, Phys. Status Solidi B **198**, 23 (1996).
[38] N. E. Christensen, J. Kudrnovský, and C. O. Rodriguez (private communication).